# Zero-phonon recombination spectra of donor-acceptor pairs in GaP and ZnSe: Model-impurity-potential approach

S. Munnix and E. Kartheuser
*Institut de Physique, Université de Liège, Belgium*
(Received 26 March 1982)

The influence of central-cell corrections on electron-hole recombination energies of donor-acceptor (DA) pairs in III-V and II-VI semiconductors is investigated. A variational treatment of the DA complex is developed in the framework of the effective-mass theory, including the effects of interaction between the charge carriers and the longitudinal-optical phonons within the static approximation. The effective-mass Hamiltonian of the DA pair, based on Fröhlich's continuum theory, allows for central-cell corrections by means of a suitable impurity model potential adjusted to experiment in the case of isolated impurities. The orbital radii of the electron and hole wave function, its departure from spherical symmetry, and the DA-pair energy are given as a function of the donor-acceptor separation $R$. The central-cell correction is found to decrease appreciably at small $R$. The results are compared with previous theoretical work and experiments on zero-phonon spectra of DA pairs in ZnSe and in GaP. It is shown that the central-cell correction cannot be neglected in order to explain the radiative DA-pair recombination energies. The model potential adopted in the present work reproduces the general trend of the $R$-dependent electron-hole recombination energies deduced from DA-pair spectra involving dopants of various depth.

## I. INTRODUCTION

Luminescence from donor-acceptor (DA) pairs in semiconductors has been widely investigated over the last several years.[1–3] The subject is of great interest, not only because the radiative recombination of electrons and holes bound to DA pairs is one of the most important mechanisms of luminescence in semiconductors, but also because the DA-pair spectra provide a large amount of information on the chemical nature and the physical properties of the impurities involved. Recently, extremely accurate spectroscopic techniques[4–7] have allowed additional knowledge on the excitation spectra of the impurities embedded in the host crystal. The radiative electron-hole recombination energy depends on the DA separation $R$. For distant pairs, the measurements are in rather good agreement with the simple theoretical model proposed by Hopfield *et al.*[8] This model yields for the energy $h\nu$ of the emitted photon

$$h\nu = E_g - (E_A + E_D) + \frac{e^2}{\epsilon_0 R} \tag{1}$$

for the case of zero-phonon pair spectra. Here $\epsilon_0$ is the static dielectric constant, $e$ is the charge of the electron, $E_g$ is the energy of the band gap, $E_A$ and $E_D$ are the ionization energies of the isolated acceptor and donor, respectively (see Fig. 1).

However, for closer pairs, the experimental results deviate from the asymptotic law, Eq. (1), due to the increasing interaction between the constituents of the DA pair for small values of $R$. In order to improve the agreement with experiment in this range, several theoretical models have been proposed: Variational calculations have been developed to allow for the overlap between the electron and hole charge distribution,[9–11] to include electron-hole correlation,[12] or to study the effect of electron-phonon interaction[13–15] for the case of polar semiconductors, where the charge carriers may appreciably interact with the longitudinal-optical (LO) phonons.

All these models are based on the hydrogenic effective-mass theory (HEMT) and thus do not account for the chemical nature of the impurities involved in the DA pair, since the donor and the acceptor ions are assumed to produce purely Coulombic potentials. Nevertheless, whereas the optical measurements on excited impurity states[16] are reasonably well described by a Rydberg series, which is nearly impurity independent and characteristic of the host material,[17–19] the ground-state energy differs from one impurity to another and may be considerably deeper than the value expected from the hydrogenic effective-mass theory. The

 

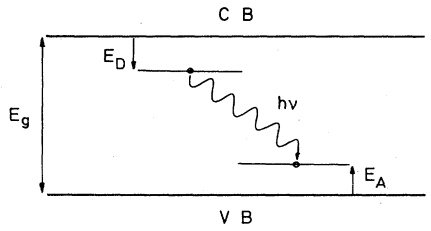


FIG. 1. Electron-hole recombination energy $h\nu$ for a donor-acceptor pair with large interimpurity separation. $E_A$ and $E_D$ are the acceptor and donor ionization energy, respectively, and $E_g$ is the band-gap energy. CB and VB denote conduction and valence bands, respectively.

reason of this discrepancy is due to the fact that in a small region around the impurity, the so-called central cell, the bound charge carriers are more sensitive to the detailed structure of the impurity, and the simple hydrogenic picture breaks down. This effect is most pronounced for the case of acceptors involved in the DA complex and particularly their ground state, where the bound charge carrier is more closely localized near the impurity than in their excited states. The difference between HEMT and experiment is generally referred to as the central-cell correction. This effect has been extensively studied in the case of isolated point defects[20,21] either by first-principles pseudopotential calculations[22–24] or by means of a phenomenological model impurity potential.[25,26]

The purpose of this work is to include central-cell effects in the DA-pair model in order to perform a systematic analysis of the zero-phonon recombination spectra of various DA pairs in polar materials such as GaP and ZnSe. We develop a variational treatment in the framework of the effective-mass theory, but use is made of a realistic model potential whose asymptotic behavior at large distances from the impurity center is Coulombic.

The outline of this paper is as follows: In Sec. II, donor and acceptor ionization energies are deduced from measurements on several DA-pair spectra.[27] In Sec. III we describe the model potential and obtain its characteristic parameters for various isolated impurities in GaP and ZnSe. Section IV is devoted to the extension of the model for the case of DA pairs. In Sec. V we compare the present results of electron-hole recombination energies to experiment and to previous theoretical work for various combinations of donors and acceptors in GaP and ZnSe.

## II. DETERMINATION OF DONOR AND ACCEPTOR IONIZATION ENERGIES FROM DA SPECTRA

The model potential described in the next section contains an impurity-dependent parameter that is selected so that the calculated ground-state binding energy of the impurity coincides with its observed value. However, the experimental determination of the impurity ionization energies is far from being trivial, and the values reported in the literature differ very often from one author to another. However, data on DA spectra[28–37] can at least partially eliminate this ambiguity. Here the detailed measurements[27] of the electron-hole recombination energies of six different DA pairs in GaP have been compiled, combining the donors O and S with the acceptors C, Zn, and Cd. Assuming that for distant DA pairs ($R \rightarrow \infty$) Eq. (1) holds, the application of a linear regression technique to the measurements carried out in the asymptotic limit leads then to the quantities $\epsilon_0$ and $h\nu_\infty = E_g - (E_A + E_D)$. We find for the static dielectric constant $\epsilon_0 = 11.1 \pm 0.1$, in agreement with the value $\epsilon_0 = 11.02$ obtained by Vink *et al.*[35] Table I shows the results for $h\nu_\infty$.

Table I enables us to eliminate the band-gap energy $E_g$ and yields the relative donor energies $E_D^O - E_D^S = 791.6$ meV and the relative acceptor energies $E_A^{Cd} - E_A^{Zn} = 32.5$ meV, $E_A^{Zn} - E_A^C = 14.6$ meV, and $E_A^{Cd} - E_A^C = 47.1$ meV. Thus only one donor and one acceptor ionization energy is needed in order to determine the whole set of binding energies. As reference energies we use the data $E_D^S = 107$ meV and $E_A^{Cd} = 102.5$ meV obtained from photoexcitation spectra[38,39] and by interimpurity recombination involving an isoelectronic trap.[40] This leads to $E_D^O = 898.6$ meV, a value slightly larger than that previously deduced[35] from ir absorption measurements.[41] Furthermore, the above three relations for the acceptor ionization energies are then satisfied for $E_A^{Zn} = 70$ meV and $E_A^C = 55.4$ meV. From these results and Table I we obtain for the energy of the indirect band gap in GaP the value

TABLE I. Electron-hole recombination energies $h\nu_\infty$ (eV) for six different dopants in GaP.

| | | Acceptors | | |
|---|---|---|---|---|
| | | C | Zn | Cd |
| Donors | O | 1.3966 | 1.3820[a] | 1.3495[a] |
| | S | 2.1882 | 2.1736 | 2.1411 |

[a]Reference 30.

$E_g = 2.3506$ eV. Note that the knowledge of $E_g$ allows the determination of the exciton binding energy $E_x$ from the more accurate measurements[42] of the energy $E_g - E_x = 2.3285$ eV required to create a free exciton. The above value of $E_g$ yields $E_x = 22.1$ meV, in excellent agreement with recently published data.[39,43,44]

In the case of ZnSe, detailed measurements[36] that involve the Li acceptor combined with the donors Al, Ga, and In are available. The values for $\epsilon_0$ and $h\nu_\infty$ obtained by fitting Eq. (1) to experiment are listed in Table II. For further calculations we have chosen $\epsilon_0 = 9.42$.[15] In the case of ZnSe, only three spectra were available, and therefore the above-mentioned procedure could not be applied here. However, the ionization energies deduced from radiative recombination of excitons bound to neutral donors[37] $E_D^{\mathrm{Al}} = 26.3$ meV, $E_D^{\mathrm{Ga}} = 27.9$ meV, and $E_D^{\mathrm{In}} = 28.9$ meV are consistent with the values for $h\nu_\infty$ shown in Table II for $E_A^{\mathrm{Li}} = 114$ meV and $E_g = 2.825$ eV.

## III. FORMALISM FOR A SINGLE IMPURITY CENTER

In polar semiconductors the movement of an electron is best described in the framework of Fröhlich's continuum model,[45] which allows for the interaction between the charge carriers and the LO phonons, i.e., the "polaron model." Extensive work has been devoted to the problem of a polaron bound by a Coulomb potential, and analytic solutions are obtained in the limiting cases when the LO-phonon energy $\hbar\omega$ is much smaller or much larger than the effective Rydberg $R^*$ associated with the impurity center.[46] For the dopants considered here, it can be shown that the electronic orbital time $\tau_0$ is, in fact, small compared to the period of the lattice vibrations $\tau_p = 2\pi/\omega$, associated with LO phonons. In this case, the lattice "feels" merely the mean electronic charge distribution rather than the instantaneous electron position, and the "adiabatic approximation" or Born-Oppenheimer approximation is most appropriate.[47] Indeed, a rough estimate of the orbital time can be obtained from the electron binding energy $E_i$ by using a Bohr-type model. This yields $\tau_0 \simeq \hbar/2E_i$. The results for the dopants in GaP and ZnSe are given in Table III and compared to $\tau_p$.

From this we may conclude that the limiting case is valid here. Within the adiabatic approximation[47,48] for the particle-lattice interaction, the effective-mass Hamiltonian of a donor-impurity center can be written as

$$H = -\frac{\hbar^2}{2m}\nabla^2 - \frac{e^2}{\epsilon_0 r} + V_{cc}(r) - \frac{1}{2}\sum_{\vec{k}} \frac{|V_k|^2}{\hbar\omega}(\rho_{\vec{k}}^* e^{i\vec{k}\cdot\vec{r}} + \rho_{\vec{k}} e^{-i\vec{k}\cdot\vec{r}}) , \tag{2}$$

where $\vec{r}$ denotes the position of the electron (hole), the donor (acceptor) impurity being taken as origin of the coordinate axes. The first term represents the kinetic energy of the electron (hole) with band mass $m_e$ ($m_h$) and charge $-e$ ($e$). Note that due to central-cell effect, the Coulomb potential felt by the electron is now modified by adding a correction $V_{cc}(r)$. The quantity $|V_k|^2$ is a measure for the strength of the interaction between the electron (hole) and the LO phonons of wave vector $\vec{k}$. Following Fröhlich,[45] we have

$$|V_k|^2 = \frac{e^2}{k^2}\frac{2\pi\hbar\omega}{V}\left[\frac{1}{\epsilon_\infty} - \frac{1}{\epsilon_0}\right] , \tag{3}$$

which can also be written

$$|V_k|^2 = \frac{4\pi\alpha_0}{V}(\hbar\omega)^2\left[\frac{\hbar}{2m\omega}\right]^{1/2}\frac{1}{k^2} , \tag{4}$$

where $\alpha_0$ is the electron (hole) LO-phonon coupling

TABLE II. Electron-hole recombination energies $h\nu_\infty$ (eV) and static dielectric constant $\epsilon_0$ obtained from DA-pair spectra in ZnSe.

| | | Donors | | |
|---|---|---|---|---|
| | | Al | Ga | In |
| Acceptor Li | $h\nu_\infty$ | 2.6847 | 2.6829 | 2.6825 |
| | $\epsilon_0$ | 9.45 | 9.39 | 9.42 |

TABLE III. Comparison between the period of LO phonons $\tau_p$ and the electronic orbital period $\tau_0$ for various dopants in ZnSe and GaP. $\tau_0$ and $\tau_p$ are measured in units of $10^{-14}$ sec.

| ZnSe | Al | Ga | In | Li | |
|---|---|---|---|---|---|
| $\tau_0$ | 7.9 | 7.4 | 7.2 | 1.8 | |
| $\tau_p$ | 13.5[a] | | | | |
| **GaP** | **Zn** | **C** | **Cd** | **S** | **O** |
| $\tau_0$ | 3.3 | 4.5 | 2.0 | 1.9 | 0.23 |
| $\tau_p$ | 8.3[a] | | | | |

[a]Reference 49.

constant

$$\alpha_0=\frac{1}{2}\frac{e^2/(\hbar/2m\omega)^{1/2}}{\hbar\omega}\left[\frac{1}{\epsilon_\infty}-\frac{1}{\epsilon_0}\right]. \quad (5)$$

Here $V$ is the volume of the crystal and $\epsilon_\infty$ the high-frequency dielectric constant. In this approximation, the source of the lattice polarization is the charge distribution described by the Fourier transform

$$\rho_{\vec{k}}=\int d\vec{r}\,|\varphi(\vec{r})|^2 e^{i\vec{k}\cdot\vec{r}}$$

or (6)

$$\rho_{\vec{k}}=\langle\varphi(\vec{r})|e^{i\vec{k}\cdot\vec{r}}|\varphi(\vec{r})\rangle\ ,$$

where the wave function $\varphi(\vec{r})$ is a solution of the Schrödinger equation

$$H\varphi(\vec{r})=E\varphi(\vec{r})\ . \quad (7)$$

In view of the application to the more complex DA pair in the next section we now search for an analytic solution of the integro-differential equation (7). This can be achieved by choosing a trial function for $\varphi(\vec{r})$ whose parameters are determined by a variational method. For the donors (and acceptors) considered here, the most reasonable choice for the ground-state wave function $\varphi(\vec{r})$ is a hydrogeniclike trial function

$$\varphi(\vec{r})=(\pi a^3)^{-1/2}e^{-r/a}\ , \quad (8)$$

whose orbital radius $a$ is taken as a variational parameter. Let us first neglect the central-cell correction [$V_{cc}(r)=0$]. Minimizing the expectation value $\langle\varphi(\vec{r})|H|\varphi(\vec{r})\rangle$ with respect to the variational parameter $a$ yields then for the ground-state energy the simple expression

$$E_0=-\frac{1}{2}\frac{me^4}{\hbar^2}\left[\frac{11}{16\epsilon_0}+\frac{5}{16\epsilon_\infty}\right]^2. \quad (9)$$

Thus allowing for the electron–LO-phonon interaction results in a modification of the Rydberg screening factor from $1/\epsilon_\infty$ to

$$\frac{1}{\epsilon}=\frac{11}{16\epsilon_0}+\frac{5}{16\epsilon_\infty}\ . \quad (10)$$

For instance, in the case of shallow donors in ZnSe (see Table IV) one obtains for the ground-state energy the values $-58.48$ and $-33.57$ meV, respectively, without and with the electron-phonon interaction. In order to compare with the measured ionization energies of donors in ZnSe (see Table V) one must subtract from $E_0$ the energy of a free polaron $-\alpha_0\hbar\omega$ when electron-phonon interaction is included. Although the value $-19.923$ meV obtained in this manner is close to experiment, there remains a slight discrepancy. This is not surprising, because the ground-state energy depends on the details of the potential felt by the electron in the immediate vicinity of the impurity, the so-called central cell. A simple Coulomb potential does not account for this feature and yields impurity-independent ionization energies. The difference between the HEMT and experiment is usually referred to as the central-cell energy. A rigorous treatment of this correction can only be achieved by first-principles calculations, including the detailed electronic structure of the host crystal as well as of the impurity ion.[22–24] However, these calculations require heavy numerical computations and their extension to more elaborate systems, such as DA pairs, would be quite complex. The problem can be dealt with in a more tractable manner by simulating the effect of the impurity by means of an analytic short-range potential. The model potential adopted here accounts for the following features: the relaxation of the electron gas due to the excess charge of the impurity and the modification of the ion core due to the replacement of the host ion by the impurity ion.

The first requirement can be fulfilled if allowance is made for the wave-number dependence of the dielectric constant.[50] The Coulomb potential is written as a Fourier expansion

TABLE IV. List of material parameters. $\epsilon_0$ and $\epsilon_\infty$ are the static and optical dielectric constant, respectively, $m_e$ ($m_h$) is the electron (hole) band mass expressed in units of the free electron mass, $\hbar\omega$ is the LO-phonon energy, and $\alpha_e$ ($\alpha_h$) is the electron (hole) LO-phonon coupling constant.

| | $\epsilon_0$ | $\epsilon_\infty$[a] | $m_e$[a] | $m_h$[a] | $\hbar\omega$ (meV)[b] | $\alpha_e$[b] | $\alpha_h$[b] |
|---|---|---|---|---|---|---|---|
| GaP | 11.02 | 9.09 | 0.365 | 0.67 | 49.97 | 0.192 | 0.260 |
| ZnSe | 9.42 | 6.10 | 0.16 | 0.52 | 30.50 | 0.448 | 0.880 |

[a]Reference 15.
[b]Reference 49.

TABLE V. Parameters for dopants in GaP and ZnSe. Ionization energies $E_i$, orbital radii $a$, and model potential parameters $K'$ and $\lambda$ for various isolated impurities. $E_i-E_i^R$ and $E_i^R-E_i^{\mathrm{HEMT}}$ are the contributions due to the short-range potential and the screened potential, respectively.

| Host crystal | Impurity | $E_i$ (meV) | $a$ (Å) | $K'$ (Å$^{-1}$) | $\lambda$ | $E_i-E_i^R$ (meV) | $E_i^R-E_i^{\mathrm{HEMT}}$ (meV) |
|---|---|---|---|---|---|---|---|
| GaP | Donors S | 107.0 | 2.33 | 1.246 | 1 | 65.7 | 5.4 |
| | O | 898.6 | 1.35 | 0.861 | 1 | 857.3 | 5.4 |
| | HEMT | 35.9 | 15.00 | 1.916 | −1 | | |
| | Acceptors C | 55.4 | 10.86 | 1.194 | −1 | −65.3 | 48.4 |
| | Zn | 70.0 | 8.51 | 1.780 | −1 | −50.7 | 48.4 |
| | Cd | 102.5 | 5.24 | 5.281 | −1 | −18.2 | 48.4 |
| | HEMT | 72.3 | 8.20 | 1.916 | −1 | | |
| ZnSe | Acceptors Li | 114.0 | 5.53 | 5.267 | 1 | −6.3 | 38.0 |
| | HEMT | 82.3 | 8.20 | 2.074 | −1 | | |
| | Donors Al | 26.3 | 19.55 | 0.676 | 1 | 5.8 | 0.5 |
| | Ga | 27.9 | 18.41 | 0.626 | 1 | 7.4 | 0.5 |
| | In | 28.9 | 17.76 | 0.603 | 1 | 8.6 | 0.5 |
| | HEMT | 19.9 | 26.70 | 2.074 | −1 | | |

$$V(r)=-4\pi e^2\int\frac{d\vec{q}\,e^{i\vec{q}\cdot\vec{r}}}{\epsilon_\infty(q)q^2}\,, \tag{11}$$

where $\epsilon_\infty(q)$ is the optical dielectric function of the host crystal.

Dispersion curves for $\epsilon_\infty(q)$ have been computed from first principles for several semiconductors including ZnSe and GaP.[51,52] The above numerical results can be fitted by the analytic expression

$$\epsilon_\infty(q)=\epsilon_\infty\frac{q^2+K^2}{\epsilon_\infty q^2+K^2}\,, \tag{12}$$

where $K$ is adjusted for each material. We find for ZnSe and GaP the values 2.074 and 1.976 Å$^{-1}$, respectively.

In order to satisfy the second requirement, an additional short-range potential with parameter $K'$ is introduced. Inserting Eq. (12) in Eq. (11) we then obtain

$$V(r)=-\frac{e^2}{\epsilon_\infty r}[1+(\epsilon_\infty-1)(e^{-Kr}+\lambda e^{-K'r})]\,, \tag{13}$$

where $\lambda$ takes the values $\pm1$. Thus

$$V(r)=-\frac{e^2}{\epsilon_\infty r}+V_{\mathrm{cc}}(r)\,, \tag{14}$$

with

$$V_{\mathrm{cc}}(r)=-\frac{\epsilon_\infty-1}{\epsilon_\infty}\frac{e^2}{r}(e^{-Kr}+\lambda e^{-K'r})\,. \tag{15}$$

A similar central-cell potential

$$V_{\mathrm{cc}}(r)=-\frac{\epsilon_\infty-1}{\epsilon_\infty}\frac{e^2}{r}(2e^{-Kr}-e^{-\alpha' r}) \tag{16}$$

has been applied with success to excited state spectra of group-III acceptors in Ge and Si.[26]

The present potential [Eq. (15)] has the same exponential behavior as that given in Eq. (16). It leads to the model potential including only the relaxation of the electron gas in the limiting case $K'\to\infty$ instead of $\alpha'=K$ as in Ref. 26. On the other hand, allowing for $\lambda=\pm1$ in Eq. (15), the model potential used here enables the treatment of the various impurities involved in the DA spectra studied in the next section. Finally, the present semiempirical potential yields the result obtained in the framework of the HEMT for $\lambda=-1$ and $K'=K$.

The parameter $K'$ and the value $\lambda=\pm1$ are now selected by adjusting the theoretical result for the ionization energy

$$E_i=\langle\varphi(\vec{r})\,|\,H\,|\,\varphi(\vec{r})\rangle_v+\alpha_0\hbar\omega \tag{17}$$

to the experimental data compiled in Sec. II. Here the quantity $\langle\varphi(\vec{r})\,|\,H\,|\,\varphi(\vec{r})\rangle_v$ corresponds to the variational result obtained from Eqs. (2), (6), (8), and (15) by minimizing

$$\begin{aligned}\langle\varphi(\vec{r})\,|\,H\,|\,\varphi(\vec{r})\rangle&=\frac{\hbar^2}{2ma^2}-\frac{e^2}{a}\left[\frac{11}{16\epsilon_0}+\frac{5}{16\epsilon_\infty}\right]\\&\quad-\frac{4e^2}{a}\left[1-\frac{1}{\epsilon_\infty}\right]\left[\frac{1}{(Ka+2)^2}+\frac{\lambda}{(K'a+2)^2}\right]\end{aligned} \tag{18}$$

with respect to the orbital radius $a$.

To illustrate the procedure adopted here in order

to obtain the parameter $K'$, let us consider, for instance, the case of donors in ZnSe. In this case the values $m_e$, $\epsilon_0$, $\epsilon_\infty$ (cf. Table IV), and $K=1.916$ are the input parameters. The variational results for $E_i$ as a function of $K'$ are shown in Fig. 2. The values $E_i^R=20.496$ meV (dotted-dashed horizontal line in Fig. 2) and $E_i^{\rm HEMT}=19.923$ meV (dashed horizontal line in Fig. 2) are obtained for $K'=\infty$ and $K'=K$, respectively, with $\lambda=-1$. Note that the experimental results for the ionization energies of the donors In, Ga, and Al studied here (solid horizontal lines in Fig. 2) all require $\lambda=+1$. The same procedure has been applied to acceptors in ZnSe and to donors and acceptors in GaP and the results for $K'$, $\lambda$, and the orbital radius $a$ are given in Table V. Figure 2 clearly demonstrates the effect of the short-range potential measured by $E_i^D-E_i^R$, as compared to the effect produced by a screened potential, i.e., $E_i^R-E_i^{\rm HEMT}$, on the ionization energy of a given donor $E_i^D$ in ZnSe. In the two last columns of Table V, we show the results for the impurities studied in this work. As shall be seen in Sec. V, the very large short-range contribution obtained for the oxygen donor in GaP will greatly affect the DA-pair energy for the case of GaP(O,C).

## IV. FORMALISM FOR THE DONOR-ACCEPTOR PAIR

The extension of the formalism developed in the preceding section to the DA pair is now straightforward. The Hamiltonian of the system is written as a sum of two parts:

$$H=H_0+H_{\rm cc}\ . \tag{19}$$

Here, $H_0$ is the effective-mass Hamiltonian of the donor-acceptor pair including electron–LO-phonon interaction within the adiabatic approximation[15]

$$H_0=-\frac{\hbar^2}{2m_e}\nabla_e^2-\frac{\hbar^2}{2m_h}\nabla_h^2+\frac{e^2}{\epsilon_0}\left[\frac{1}{|\vec{r}_e-\vec{R}|}+\frac{1}{r_h}-\frac{1}{r_e}-\frac{1}{|\vec{r}_h-\vec{R}|}-\frac{1}{R}\right]-\frac{e^2}{\epsilon_\infty|\vec{r}_e-\vec{r}_h|}$$
$$-\tfrac{1}{2}\sum_{\vec{k}}\frac{|V_k|^2}{\hbar\omega}[\rho^*_{\vec{k}}(e^{i\vec{k}\cdot\vec{r}_e}-e^{i\vec{k}\cdot\vec{r}_h})+\rho_{\vec{k}}(e^{-i\vec{k}\cdot\vec{r}_e}-e^{-i\vec{k}\cdot\vec{r}_h})]\ , \tag{20}$$

where $\vec{R}$, $\vec{r}_e$, and $\vec{r}_h$ denote the positions of the acceptor center $A^-$, of the electron $e$, and of the hole $h$, respectively, when the donor impurity $D^+$ is taken as the origin of the coordinate axes (see Fig. 3). The source of the ionic polarization is now given by the Fourier transform

$$\rho_{\vec{k}}=\langle F_R(\vec{r}_e,\vec{r}_h)\,|\,(e^{i\vec{k}\cdot\vec{r}_e}-e^{i\vec{k}\cdot\vec{r}_h})F_R(\vec{r}_e,\vec{r}_h)\rangle \tag{21}$$

in terms of the electronic part $F_R(\vec{r}_e,\vec{r}_h)$ of the DA-pair envelope function.

The second contribution $H_{\rm cc}$ represents the central-cell correction

$$H_{\rm cc}=V_D(r_e)-V_D(r_h)$$
$$-V_A(|\vec{r}_e-\vec{R}|)+V_A(|\vec{r}_h-\vec{R}|)\ , \tag{22}$$

described by means of the short-range potential (15). Here, the subscripts $D$ and $A$ refer to the particular value of $K'$ and associated with the donor and acceptor impurity, respectively. As in Sec. III, we now proceed with the variational calculation of the DA-pair ground-state energy. Neglecting electron-hole correlation effects,[12] we choose a product of one-particle functions for the trial ansatz:

$$F_R(\vec{r}_e,\vec{r}_h)=\varphi_e(\vec{r}_e)\rho_h(\vec{r}_h)\ . \tag{23}$$

For distant pairs, the Coulomb interactions between the donor and acceptor impurities are weak, and the wave functions $\varphi_e(\vec{r}_e)$ and $\varphi_h(\vec{r}_h)$ are almost spherical $1s$ functions (8). However, for close DA pairs, these Coulomb interactions give rise to a deviation from spherical symmetry, which may be accounted for by adding a term of $p$ symmetry to the $1s$ trial function. This leads to

$$\varphi_e(\vec{r}_e)=\frac{a^{-3/2}}{\pi^{1/2}(1+s^2)^{1/2}}e^{-r_e/a}\times\left[1+s\frac{r_e}{a}\cos\theta_e\right]\ , \tag{24}$$

$$\varphi_h(\vec{r}_h)=\frac{\alpha^{-3/2}}{\pi^{1/2}(1+\sigma^2)^{1/2}}e^{-|\vec{r}_h-\vec{R}|/\alpha}\times\left[1+\sigma\frac{|\vec{r}_h-\vec{R}|}{\alpha}\cos\theta_h\right]\ , \tag{25}$$

where $\theta_e$ and $\theta_h$ are defined in Fig. 3 and $a$ and $\alpha$ characterize the size of the orbitals, whereas $s$ and $\sigma$ allow for nonsphericity of the electron and hole charge densities, respectively. An upper bound to the DA-pair ground-state energy can now be ob-

tained by minimizing the expectation value

$$E(R)=\langle F_R(\vec{r}_e,\vec{r}_h)\,|\,H_0\,|\,F_R(\vec{r}_e,\vec{r}_h)\rangle + \langle F_R(\vec{r}_e,\vec{r}_h)\,|\,H_{cc}\,|\,F_R(\vec{r}_e,\vec{r}_h)\rangle \quad (26)$$

with respect to the variational parameters $a$, $\alpha$, $s$, and $\sigma$. Detailed analytic expressions for the quantity

$$\langle F_R(\vec{r}_e,\vec{r}_h)\,|\,H_0\,|\,F_R(\vec{r}_e,\vec{r}_h)\rangle$$

are given in Ref. 15 and are not reproduced here. For the second contribution in (26) we obtain

$$\langle F_R(\vec{r}_e,\vec{r}_h)\,|\,H_{cc}\,|\,F_R(\vec{r}_e,\vec{r}_h)\rangle = -\left[1-\frac{1}{\epsilon_\infty}\right][I(a,s,K)+\lambda_D I(a,s,K'_D)+I(\alpha,\sigma,K)-T(a,s,K)+\lambda_A I(\alpha,\sigma,K'_A)-T(\alpha,-\sigma,K) -\lambda_A T(a,s,K'_A)-\lambda_D T(\alpha,-\sigma,K'_D)] \quad (27)$$

with

$$I(a,s,K)=\frac{4}{a(1+s^2)(Ka+2)^2}\times\left[1+\frac{2s^2}{(Ka+2)^2}\right] \quad (28)$$

and

$$T(a,s,K)=\int\frac{d\vec{r}\,e^{-2r/a_e-K\,|\,\vec{r}-\vec{R}\,|}}{\pi a^3(1+s^2)\,|\,\vec{r}-\vec{R}\,|}\times\left[1+s\frac{r}{a}\cos\theta\right]^2. \quad (29)$$

Detailed expressions for $T(a,s,k)$ are given in the Appendix. The variational results for the orbital radii $a$ and $\alpha$, the deformation parameters $s$ and $\sigma$ and the energy $E$ are given as a function of the donor-acceptor separation $R$ in Table VI for various dopants in GaP and for ZnSe doped with In and Li.

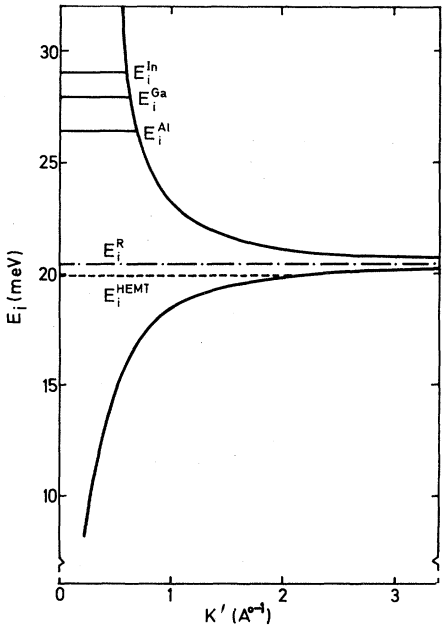


FIG. 2. Determination of the model potential parameter $K'$ for donors in ZnSe: Variational results for the ionization energy $E_i$ as a function of the model potential parameter $K'$. The upper and lower curves belong to $\lambda=\pm1$, respectively. Solid horizontal lines indicate the ionization energies and the corresponding values for $K'$ (column six in Table V) related to the In, Ga, and Al donors, respectively. Dashed horizontal line shows the value obtained in the framework of the HEMT ($K'=K$), and dotted-dashed horizontal line represents the result for $E_i$ obtained by including only the relaxation of the electron gas in the model potential ($K'\to\infty$).

## V. DISCUSSION AND COMPARISON WITH EXPERIMENT

In order to demonstrate the effect of the chemical shift, the formalism developed in the preceding section has been applied to pair spectra resulting from three different kinds of dopants in polar semiconductors: the shallow dopants In and Li in ZnSe, the moderately deep dopants such as S and

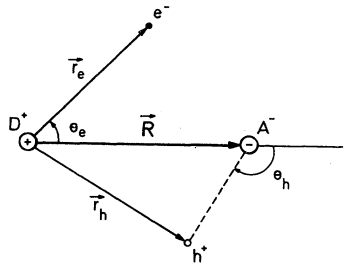


FIG. 3. Molecular model of the donor-acceptor pair. The coordinates of the electron $e$, the positive hole $h$, and the acceptor $A^-$ are chosen with reference to the donor $D^+$.

TABLE VI. Variational results as a function of the pair separation $R$ for various dopants in ZnSe and GaP: the first column shows the host material and its dopants (inside parentheses); columns 3–7 show the electron and hole orbital radii ($a$ and $\alpha$), the electron and hole $s$-$p$ mixing parameters ($s$ and $\sigma$), and energy $E(R)$ of the DA pair. The last column gives the central-cell energy $E_{cc}(R)$ obtained from the present results $E(R)$ by substracting the HEMT value (Ref. 15).

| | $R$ (Å) | $a$ (Å) | $\alpha$ (Å) | $s$ | $\sigma$ | $E(R)$ (meV) | $E_{cc}(R)$ (meV) |
|---|---|---|---|---|---|---|---|
| GaP(S,Zn) | 35 | 2.31 | 8.50 | −0.000 | 0.003 | −199.3 | 67.2 |
| | 30 | 2.30 | 8.50 | −0.000 | 0.008 | −199.2 | 67.1 |
| | 25 | 2.30 | 8.50 | −0.000 | 0.019 | −199.1 | 66.9 |
| | 20 | 2.30 | 8.51 | −0.001 | 0.041 | −199.9 | 66.5 |
| | 15 | 2.30 | 8.67 | −0.002 | 0.079 | −202.2 | 63.2 |
| | 10 | 2.30 | 9.38 | −0.015 | 0.124 | −213.6 | 48.1 |
| | 5 | 21.65 | 21.46 | −0.052 | 0.067 | −290.5 | 0.2 |
| GaP(S,Cd) | 35 | 2.31 | 5.24 | −0.000 | 0.000 | −231.8 | 99.7 |
| | 30 | 2.31 | 5.24 | −0.000 | 0.000 | −231.8 | 99.7 |
| | 25 | 2.31 | 5.24 | −0.000 | 0.001 | −231.8 | 99.6 |
| | 20 | 2.31 | 5.22 | −0.000 | 0.006 | −232.7 | 99.3 |
| | 15 | 2.31 | 5.17 | −0.001 | 0.025 | −233.8 | 94.8 |
| | 10 | 2.29 | 5.27 | −0.005 | 0.082 | −240.9 | 75.4 |
| | 5 | 20.03 | 18.62 | −0.056 | 0.073 | −289.8 | 0.9 |
| GaP(C,O) | 35 | 1.35 | 10.86 | −0.000 | 0.011 | 976.3 | 844.2 |
| | 30 | 1.35 | 10.86 | −0.000 | 0.024 | 976.3 | 844.2 |
| | 25 | 1.35 | 10.87 | −0.000 | 0.044 | 976.0 | 843.8 |
| | 20 | 1.35 | 11.00 | −0.000 | 0.073 | 975.5 | 842.1 |
| | 15 | 1.35 | 11.41 | −0.000 | 0.111 | 975.1 | 836.1 |
| | 10 | 1.35 | 12.38 | −0.002 | 0.140 | 975.3 | 809.8 |
| | 8 | 1.35 | 12.91 | −0.006 | 0.141 | 977.2 | 778.3 |
| | 5 | 1.36 | 13.74 | −0.001 | 0.115 | 995.1 | 704.4 |
| ZnSe(In,Li) | 35 | 18.23 | 5.59 | −0.047 | 0.006 | −184.6 | 41.2 |
| | 30 | 18.56 | 5.58 | −0.064 | 0.008 | −184.7 | 40.7 |
| | 25 | 19.13 | 5.57 | −0.084 | 0.012 | −185.1 | 39.8 |
| | 20 | 19.90 | 5.54 | −0.100 | 0.022 | −185.7 | 37.5 |
| | 15 | 20.65 | 5.57 | −0.093 | 0.055 | −190.2 | 33.5 |
| | 10 | 22.20 | 7.71 | −0.056 | 0.123 | −216.0 | 25.6 |
| | 5 | 33.45 | 28.86 | −0.036 | 0.058 | −335.6 | −2.7 |

Zn and S and Cd in GaP, and deep impurities such as O combined with C in GaP. From the results in Table VI, the following general trends can be deduced for all DA pairs studied here: The orbital radii $a$ and $\alpha$ of the electron and hole, respectively, increase with decreasing DA-pair separation $R$. This is caused by the electrostatic interaction experienced by the charge carriers. Indeed, as the impurities are brought together, the electron "feels" the repulsive action of the negatively charged acceptor ion more and more, while the hole experiences the repulsion by the positively charged donor ion. At the same time, this leads to an enhancement of the departure from spherical symmetry along the DA-pair axis and thus causes an increase of the deformation parameters $s$ and $\sigma$.

In the last column of Table VI we have listed the central-cell correction $E_{cc}(R)$ to the DA-pair energy, i.e., the difference between the present result $E(R)$ and that obtained in the framework of the hydrogenic effective-mass approximation.[15]

The present results show a strong decrease of the central-cell effect with decreasing DA-pair separation $R$. For very small values of $R$ ($R \sim 5$ Å), this correction nearly vanishes, and the variational parameters $a$, $\alpha$, and $\sigma$ obtained in the present work are close to those obtained neglecting central-cell effects,[15] except for deep dopants such as oxygen. This behavior is easily understood from the enhancement of the orbital radii when $R$ is lowered. As a consequence the electron (hole) charge distribution is spread out over larger distances from the donor (acceptor) impurity at small $R$ values, and thus the probability of finding the electron (hole) in the central-cell region decreases when the DA-pair separation diminishes.

Let us now discuss in more detail the differences between shallow dopants and deep dopants: Although the dopants In and Li in ZnSe (see Tables V and VI) can be considered as fairly shallow impurities, we see from the present results that the central-cell contribution to the DA-pair energy still ranges from 0% up to 22% for $R$ equal to 5 and 35 Å, respectively. In the other extreme, the case of deep centers such as O and C in GaP (see Tables V and VI), this correction accounts for 86% to the total energy at large $R$ and only decreases for $R$ below 10 Å due to the very small orbital radius of the electron bound to the oxygen donor impurity.

Furthermore, we note that for shallow dopants (In and C) the orbital radii increase smoothly over the whole range of $R$ values listed, whereas for deeper impurities (Li and O), they remain constant over a wide range of $R$ values, increasing abruptly below a given impurity separation which is smaller the deeper the impurities are. This can be explained from the difference in effective Bohr radii for the isolated impurities (see Table V): For instance, in the case of ZnSe, the donor orbital radius (17.76 Å for the In donor) being larger than the acceptor orbital radius (5.53 Å for the Li acceptor), the electron-acceptor repulsion responsible for the increase in orbital radius, sets up at much larger values for $R$ than the hole-donor interaction.

Finally, it can be seen from Table VI that the deformation parameters $s$ or $\sigma$ pass through a maximum value at a critical DA-pair separation $R_c$. This critical pair separation is reached when the electron (hole) charge density starts to "embrace" the acceptor (donor) ion. We see from the present results that $R_c$ is larger for shallow dopants ($R_c = 20$ Å for In) than for the deeper impurity ($R_c = 10$ Å for Li) as expected. In summary, the general trends sketched above are more and more pronounced as we turn our attention to DA pairs involving deeper impurities.

The $R$ dependence of the DA-pair energy $E(R)$ obtained in the present work is best compared to experiment by analyzing the deviation $\Delta E(R)$ from the ideal $1/R$ law, Eq. (1). Thus we define

$$\Delta E(R) \equiv h\nu(R) - \frac{e^2}{\epsilon_0 R} = E_g + E(R) \,. \tag{30}$$

In order to demonstrate the effect of the depth of the dopant on the $R$ dependence of the electron-hole recombination energy $h\nu(R)$ we have plotted the measurements versus $R$ for three different DA pairs in GaP (see Fig. 4). Here the asymptotic value $\Delta E(R=\infty) = E_g - E_A - E_D$ has been taken as origin for the energy scale, and the physical parameters given in the previous sections have been used.

Figure 4 clearly exhibits the departure of the experimental results from the ideal $1/R$ law, Eq. (1). The distance $R$ at which this deviation sets on strongly depends on the depth of the dopants involved in the pair spectra. As we shall see in the following, the present theoretical model accounts for the above deviations and their dependence on the depth of the impurity.

In Figs. 5–8, we have plotted our theoretical results for $\Delta E$ (solid curves) versus $R$ for different dopants in ZnSe and GaP. In each case a comparison has been made to experiment (dotted curves) and to the corresponding theoretical results $\Delta E_0(R)$ obtained in the framework of the HEMT (Ref. 15) adjusted to experiment at $R = \infty$ (dashed curves).[53]

For the three combinations of dopants investigated in ZnSe, the DA-pair energy is almost the same. Therefore we only display the results for one pair spectra.[54]

As seen from Figs. 5–8, the variational calculation adopted here yields an upper limit to the measurements in the whole range of $R$ values, as required by such a procedure while the HEMT curves lie below the experimental data for close pairs. This improvement is clearly due to the inclusion of the $R$-dependent central-cell effect. Indeed, as discussed above, the central-cell contribution to the DA-pair energy decreases with $R$ and thus leads to a continuous raise of the quantity $\Delta E$ when the donor and acceptor impurities become closer and closer together. The difference between

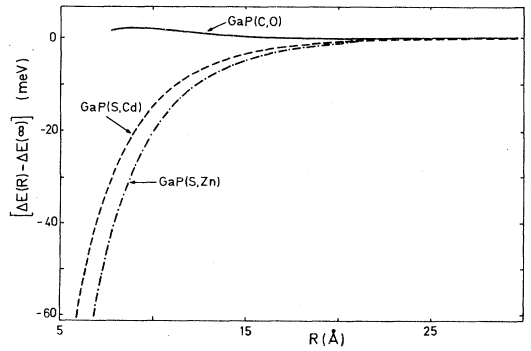


FIG. 4. Experimental results for the departure of the electron-hole recombination energy $\Delta E = h\nu(R) - e^2/\epsilon_0 R$ from the ideal $1/R$ law. Measurements for various dopants in GaP (Ref. 27) taking $h\nu_\infty = \Delta E(\infty)$ as origin for the energy scale and for $\epsilon_0 = 11.01$.

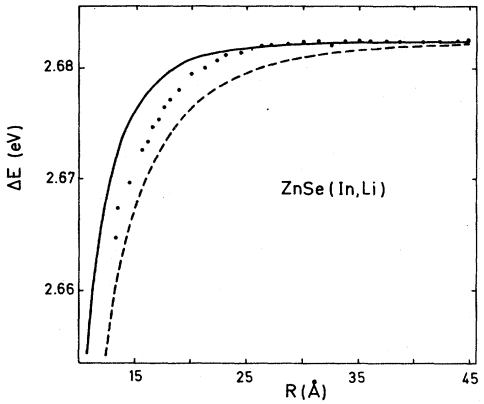


FIG. 5. Deviation $[\Delta E = E(R) + E_g]$ of the DA-pair energy from the asymptotic value $h\nu_\infty = E_g - E_A - E_D$ ($E_A$ and $E_D$ are the acceptor and donor ionization energy, respectively, in the case of ZnSe doped with Li and In); the points correspond to the experimental data (Ref. 36) with $\epsilon_0 = 9.42$; solid and dotted curves show the present theoretical results and those obtained from HEMT (Ref. 15), respectively.

the present work and the HEMT approach is most striking for the case of the deep DA pair GaP(C,O) (see Fig. 8) for which our theoretical results provide a quantitative agreement with experiment in a large range of $R$ values. This is related to the fact that for the DA pair GaP(C,O), the most important contribution to the pair energy is due to the short-range effect produced by the oxygen donor (up to 88% of the total energy). As a consequence, the charge carriers remain far more localized around their respective impurities, even at short interimpurity distances, than in the case of shallow DA pairs and thus interact only weakly. It follows that for GaP(C,O) the presence of the

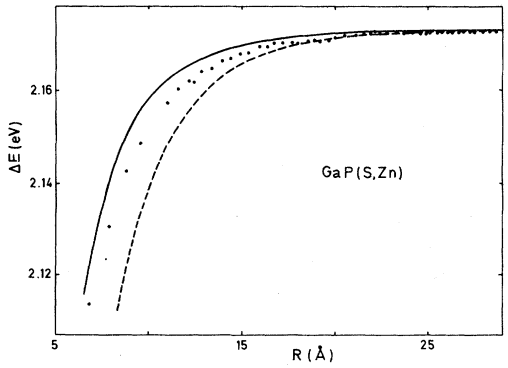


FIG. 6. Deviation $\Delta E$ vs DA-pair separation $R$ for GaP doped with S and Zn: · · · experimental results (Ref. 27), — — — HEMT (Ref. 15), — present theory.

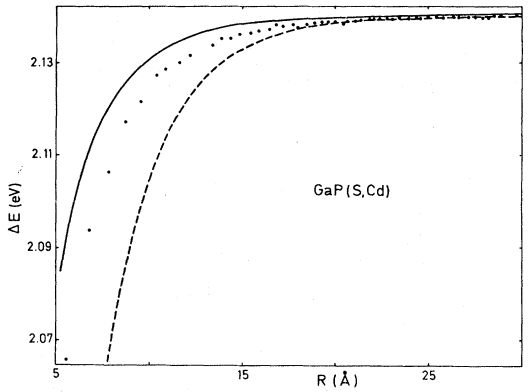


FIG. 7. Deviation $\Delta E$ vs DA-pair separation $R$ in the case of GaP doped with S and Cd: · · · experimental results (Ref. 27), — — — HEMT (Ref. 15), — present theory.

short-range contribution in the present model potential leads to a nearly constant value for $\Delta E(R)$, even for relatively close DA pairs.

At small $R$, there remains, however, a slight discrepancy between theory and experiment, which may be partially due to the breakdown of the adiabatic approximation used here in order to account for electron—LO-phonon interaction. In addition, for very close pairs, $R \sim 5$ Å, the present DA-pair model is questionable and should be replaced by a DA pair made up of an exciton bound to a dipole field created by the donor and acceptor ions. No significant improvement seems to be expected from the use of other model potentials. However, calculations made with step potentials did not yield

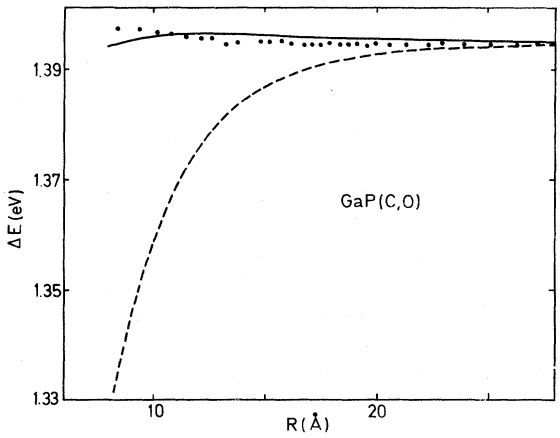


FIG. 8. Deviation $\Delta E$ vs DA-pair separation $R$ in the case of GaP doped with C and O: · · · experimental results (Ref. 27), — — — HEMT (Ref. 15), — present theory.

good agreement with experiment. On the other hand, applying[55] the potential of Eq. (16) leads to results that differ from the present calculations only by a few tenths of a meV.

## VI. CONCLUSIONS

In this paper we have studied the importance of central-cell effects on the electron-hole recombination energy for various combinations of dopants in GaP and ZnSe. The analysis of the experimental DA spectra is made in a systematic and self-consistent manner. The variational treatment is based on a model potential that includes the effect of the chemical nature of the dopants involved in the DA pair.

It is shown that the central-cell correction decreases when the donor and acceptor impurities are brought together. Whereas for distant pairs this effect contributes from 20% up to 80% to the DA-pair energy, depending on whether the impurities are shallow or deep, it almost vanishes for close pairs. The impurity-dependent departure from the ideal $1/R$ law for the electron-hole recombination energy is well described by the present model.

## ACKNOWLEDGMENTS

The authors are grateful to W. Senske and A. K. Vink for providing us detailed data on their measurements of electron-hole recombination energies versus DA-pair separation in GaP. One of us (S.M.) would like to thank the Belgian Fonds National de la Recherche Scientifique for financial support.

## APPENDIX: COMPUTATION OF THE INTEGRAL $T(a,s,k)$ IN EQ. (27)

Using the Fourier transform of $e^{-K|\vec{r}-\vec{R}|}/|\vec{r}-\vec{R}|$ the function $T(a,s,k)$ can be expressed in terms of the following integrals:

$$S_{p,m,n}(K,a)=\frac{2}{\pi}\int_0^\infty \frac{dk\,k^p \sin kR}{(k^2+K^2)^m[(a/2)^2k^2+1]^n}\,, \tag{A1}$$

$$C_{p,m,n}(K,a)=\frac{2}{\pi}\int_0^\infty \frac{dk\,k^p \cos kR}{(k^2+K^2)^m[(a/2)^2k^2+1]^n}\,. \tag{A2}$$

This yields:

$$T(a,s,K)=\frac{S_{1,1,1}(K,a)}{(1+s^2)R}+\frac{2s}{1+s^2}\frac{a}{R}T_2+\frac{s^2}{1+s^2}\frac{T_3}{R} \tag{A3}$$

with

$$T_2=\frac{1}{R}S_{1,1,3}(K,a)-C_{2,1,3}(K,a)\,, \tag{A4}$$

$$T_3=S_{1,1,1}(K,a)-\frac{3}{2}a^2S_{3,1,4}(K,a)-3\frac{a^2}{R}C_{2,1,4}(K,a)+3\frac{a^2}{R^2}S_{1,1,4}(K,a)\,. \tag{A5}$$

[1]F. Williams, Phys. Status Solidi 25, 493 (1968).
[2]P. J. Dean, *Progress in Solid State Chemistry* (Pergamon, New York, 1973), Vol. 8, p. 1.
[3]A. E. Yunovich, Fortschr. Phys. 23, 317 (1973).
[4]S. Nakashima and Y. Yamaguchi, J. Appl. Phys. 50, 4958 (1978).
[5]P. J. Wiesner, R. A. Street, and H. D. Wolf, Phys. Rev. Lett. 35, 1366 (1975).
[6]H. Tews, H. Venghaus, and P. J. Dean, Phys. Rev. B 19, 5178 (1979).
[7]W. Senske and R. A. Street, Phys. Rev. B 20, 3267 (1979).
[8]J. J. Hopfield, D. G. Thomas, and M. Gershenson, Phys. Rev. Lett. 10, 162 (1963).
[9]L. Mehrkam and F. Williams, Phys. Rev. B 6, 3753 (1972).
[10]W. Senske, M. Sondergeld, and H. J. Queisser, Phys. Status Solidi B 89, 467 (1978).
[11]R. Bindemann and K. Unger, Phys. Status Solidi B 56, 563 (1973).

[12]E. Kartheuser, A. Babcenco, and R. Evrard, Phys. Status Solidi B 109, 375 (1982).
[13]B. Stébé and G. Munschy, Phys. Status Solidi B 60, 133 (1973).
[14]E. Kiefer and W. Schröder, J. Lumin. 14, 235 (1976).
[15]E. Kartheuser, R. Evrard, and F. Williams, Phys. Rev. B 21, 648 (1980).
[16]P. Fisher and A. K. Ramdas, in *Physics of the Solid State,* edited by S. Balakrishna, M. Krishnamuri, and B. Ramachandra (Academic, London, 1969), p. 149.
[17]W. Kohn, in *Solid State Physics,* edited by F. Seitz and D. Turnbull (Academic, New York, 1957), Vol. 5, p. 257.
[18]R. A. Faulkner, Phys. Rev. 184, 713 (1969).
[19]F. Bassani, G. Iadonisi, and B. Preziosi, Rep. Prog. Phys. 37, 1099 (1974).
[20]S. T. Pantelides, Rev. Mod. Phys. 50, 797 (1978).
[21]M. Jaros, Adv. Phys. 29, 410 (1980).
[22]M. Jaros and S. F. Ross, J. Phys. C 6, 3451 (1973).
[23]G. A. Baraff and M. Schlüter, Phys. Rev. Lett. 41, 892 (1978).
[24]J. Bernholc, N. O. Lipari, and S. T. Pantelides, Phys. Rev. Lett. 41, 895 (1978).
[25]T. H. Ning and G. T. Sah, Phys. Rev. B 4, 3468 (1971).
[26]N. O. Lipari, A. Baldereschi, and M. L. W. Thewalt, Solid State Commun. 33, 277 (1980).
[27]This analysis has been made from a great number of detailed measurements on energies of the pair lines kindly communicated by A. T. Vink and W. Senske.
[28]D. G. Thomas, M. Gershenzon, and F. A. Trumbore, Phys. Rev. 133, A269 (1964).
[29]F. A. Trumbore and D. G. Thomas, Phys. Rev. 137, A1030 (1965).
[30]P. J. Dean, C. J. Frosch, and C. H. Henry, J. Appl. Phys. 39, 5631 (1968).
[31]P. J. Dean, E. G. Schönherr, and R. B. Zetterstrom, J. Appl. Phys. 41, 3474 (1970).
[32]P. J. Dean, R. A. Faulkner, and S. Kimura, Phys. Rev. B 2, 4062 (1970).
[33]P. J. Dean and M. Ilegems, J. Lumin. 4, 201 (1971).
[34]M. R. Lorenz, D. G. Petit, and S. E. Blum, Solid State Commun. 10, 705 (1972).
[35]A. T. Vink, R. L. A. Van der Heijden, and A. J. W. Van der Does de Bye, J. Lumin. 8, 105 (1973).
[36]J. L. Merz, Phys. Rev. B 9, 4593 (1974).
[37]J. L. Merz, K. Nassau, and J. W. Shiever, Phys. Rev. B 8, 1444 (1973).
[38]A. A. Kopylov and A. N. Pikhtin, Fiz. Tekh. Poluprovodn. 11, 867 (1977) [Sov. Phys.—Semicond. 11, 510 (1977)].
[39]V. Berndt, A. A. Kopylov, and A. N. Pikhtin, Fiz. Tekh. Poluprovodn. 11, 1782 (1977) [Sov. Phys.—Semicond. 11, 1044 (1977)].
[40]M. D. Sturge, A. T. Vink, and F. P. J. Kuijpers, Appl. Phys. Lett. 32, 49 (1978).
[41]A. Onton and R. C. Taylor, Phys. Rev. B 1, 2587 (1970).
[42]P. J. Dean and D. G. Thomas, Phys. Rev. 150, 690 (1966).
[43]R. Bindemann, R. Schwabe, and T. Hänsel, Phys. Status Solidi B 87, 169 (1978).
[44]R. Bindemann, H. Fischer, and K. Kreher, Phys. Status Solidi A 49, 331 (1978).
[45]H. Fröhlich, H. Pelzer, and S. Zienau, Philos. Mag. 41, 221 (1951). See also *Polarons in Ionic Crystals and Polar Semiconductors,* edited by J. T. Devreese (North-Holland, Amsterdam, 1972).
[46]For a critical discussion, see, for instance, K. Takegahara and T. Kasuya, J. Phys. Soc. Jpn. 39, 1292 (1975).
[47]V. M. Buimistrov and S. I. Pekar, Zh. Eksp. Teor. Fiz. 32, 1193 (1957) [Sov. Phys.—JETP 5, 970 (1957)].
[48]P. M. Platzmann, Phys. Rev. 125, 1961 (1962).
[49]E. Kartheuser, in *Polarons in Ionic Crystals and Polar Semiconductors,* edited by J. T. Devreese (North-Holland, Amsterdam, 1972), p. 717.
[50]J. Bernholc and S. Pantalides, Phys. Rev. B 15, 4935 (1977).
[51]J. P. Walter and M. L. Cohen, Phys. Rev. B 2, 1821 (1970).
[52]P. K. W. Vindsome and D. Richardson, J. Phys. C 4, 2650 (1971).
[53]Notice that the theoretical curve shown in Ref. 15 has been adjusted to experiment at $R=35$ Å and therefore seems to agree much better with experiment, as shown in Fig. 5.
[54]S. Munnix and E. Kartheuser, Solid State Commun. 39, 177 (1981).
[55]The present calculations have been compared with those obtained using $V_{cc}$ given by Eq. (16) in the case of GaP(S,Cd). Here the experimental value for the ionization energy of the sulfur donor can only be fitted, replacing $-e^{-\alpha' r}$ in Eq. (16) by $+e^{-\alpha' r}$.